Langevin equation for charged granular gases

David Liu, supervisor: **Dr Marco G. Mazza**
Max Planck Institute for Dynamics and Self-Organization (Ludwig Prandtl Internship 2018)

***Abstract*—The Langevin formalism provides an effective stochastic description of the self-diffusion process in viscoelastic granular gases. In the limit of slightly inelastic particle collisions, one can employ a quasi-equilibrium approximation to obtain scaled Brownian motion characterizing the single-particle trajectories. Such effective single-particle descriptions allow the quick generation of particle trajectories without requiring to run full molecular dynamics simulations or tracking experiments. Here, we extend the Langevin approach to charged granular gases, introducing a velocity-dependent dynamical friction coefficient. We find a speed dependence u^{-3} at high speeds deduced from Coulomb scattering theory that is similar to the dynamical friction coefficient found for plasmas and collisionless star systems. Comparison with molecular dynamics simulation data shows that the computed friction coefficient agrees with the theoretical form with fitted parameters. Using our theoretical expression, we discretize the Langevin equation and numerically model the predicted particle trajectories with a modified Euler-Maruyama algorithm. Both the molecular dynamics and Langevin approach show from the mean-square displacement that the charged self-diffusion process is slightly more subdiffusive compared to the neutral case.**

I. Introduction

Granular materials are ubiquitous in nature and industry. Undoubtedly the most familiar example is sand, which exhibits interesting behaviour characterstic of both liquids and solids [1]. In Space, interstellar clouds, planet rings [2] and planetary formation in protoplanetary disks all involve granular matter dynamics. A particular class of granular materials are granular gases, analogous to molecular gases in that the typical inter-particle spacing exceeds particle size. It forms a fundamental model system for collective non-equilibrium theory [3]. The defining property of granular gases is the inelastic collision interaction, as opposed to elastic collisions in molecular gases. Physically, internal microscopic degrees of freedom of the particles are ignored on a mesoscopic scale leading to energy dissipation. Realistic models incorporate a velocity-dependent restitution coefficient, called viscoelastic granular gases. Such systems exhibit density instabilities leading to clustering [4, 5], which is in stark contrast with molecular gases. Macroscopic fluxes generally appear as clusters form [6]. Dissipation also leads to continuous reduction of the total kinetic energy of the granules referred to as cooling, keeping the system away from thermal equilibrium. Furthermore, violation of ergodicity in the Boltzmann-Khinchin sense, as well as ageing, are observed for these models [7].

The Langevin formalism has been applied to study self-diffusion in granular gases, resulting in scaled Brownian motion (SBM) [8]. This is a non-stationary stochastic process which shows properties as non-ergodicity and ageing [9]. In the limit of small inelasticity, kinetic theory [6] predicts similar results for mean-squared displacements (MSD) and other correlations related to single-particle trajectories. Molecular dynamics (MD) simulations corroborate this observation and results for ensemble- and time-averaged MSD agree very well with the theoretical results as shown in literature [7, 8]. Finding such a Langevin equation describing the self-diffusion allows one to compute quantities related to single-particle statistics very quickly without resorting to expensive MD simulations.

An interesting extension of the above granular gas model is to include electric charge on the granules. Unlike its neutral counterpart, the dynamics and collective behaviour of charged granular gases are not yet well understood. Materials brought in contact may lead to charge transfer, referred to as tribocharging, and even identical materials can mutually transfer charge [10]. Collisional charging is not well understood and depends on many factors such as surface roughness and shape [11], but is an integral part of the model responsible for the acquisition of charge. It is possible that the resulting electrostatic interactions play a fundamental role in the early stages of planetary formation [12], and the formation of lightning in various circumstances [13, 14] is directly related to these charging processes. The range of the Coulomb interaction between charged granules means that particle trajectories between collision events will no longer be ballistic. This prevents the use of event-driven MD simulations and one has to resort to the full integration of the equation of motion. Experimental studies [15, 16] on real-life realization of such granular systems show collide-and-capture events, as well as orbital motion characteristic of $1/r$ potentials.

In this study, we formulate a Langevin approach to the charged granular gas and find a velocity-dependent dynamical friction coefficient. Theoretical predictions based on Coulomb scattering produce similar expressions known in plasma physics, which we compare with computed values of the dynamic friction coefficient from MD simulations. For the range of velocities available, the MD simulations agree with the functional form derived from first principles. The Langevin equation was discretized into a finite difference equation for computation, which allows comparison of the single-particle trajectories predicted by the Langevin approach with the MD trajectories. There a more subdiffusive behaviour is observed for the charged model, which agrees qualitatively with MD results.

II. Analysis

A. Langevin equation

The self-diffusion of a tracked particle can be described using Newton's equation, with the force term interpreted as a

stochastic variable

$$m\frac{d^2\mathbf{r}}{dt^2} = \mathbf{F}(t) \tag{1}$$

where $\mathbf{F}(t)$ represents all the forces (contact and ranged Coulomb interactions) the tracked particle experiences. As part of the Langevin formulation, we assume that the surrounding gas represents a homogeneous and isotropic medium. In the reference frame of the tracked particle however, the surrounding is still homogeneous but no longer isotropic; particles move with a net drift velocity $-\mathbf{u}$. This breaks the isotropy and a term along the direction of velocity is expected in $\mathbf{F}(t)$. As the system evolves, all the collisions and interactions wash out the initial condition $\mathbf{u}_0$ of a particle. Combined with this notion, we decompose the force respectively into a systematic damping and a stochastic part

$$\mathbf{F}(t) = -\gamma(u,t)\mathbf{u} + \boldsymbol{\xi}(t) \tag{2}$$

Note that this decomposition is consistent with the ensemble average $\langle \mathbf{F}(t)\rangle = \mathbf{0}$. $\langle \gamma(u,t)\mathbf{u}\rangle$ is still zero as $\gamma(u,t)$ depends only on speed in this model, and for a given speed $\mathbf{u}$ can still point in any direction. There is no preferred direction for $\boldsymbol{\xi}(t)$.

It is possible to obtain γ using $\langle \boldsymbol{u}(t)\boldsymbol{\xi}(t')\rangle_u = 0$ (which holds for any $\{t,t'\}$ since $\boldsymbol{\xi}(t)$ is random) from the inner product with (2)

$$\gamma(u,t) = -\frac{\langle \boldsymbol{u}(t)\cdot\boldsymbol{F}(t)\rangle_u}{\langle \boldsymbol{u}(t)\cdot\boldsymbol{u}(t)\rangle_u} \tag{3}$$

where the ensemble average is restricted to particles with speed u. Note the denominator will be trivially equal to $u^2(t)$.

The stochastic force or noise term is taken to be white and Gaussian with its defining autocorrelation

$$\langle \boldsymbol{\xi}(t)\cdot\boldsymbol{\xi}(t')\rangle = \Gamma(t)\delta(t-t') \tag{4}$$

which for Brownian motion is justified by the collision timescale $\tau_c \ll \tau_{obs}$, the observation timescale. In the case of self-diffusion, τ_c is not necessarily much smaller as the masses of the colliding particles are equal now, and it is not a priori clear whether the noise is white and Gaussian. However for white noise, the exact probability distribution should not matter as adding up independent noise impulses over a sufficiently long observation timescale tends to a Gaussian process by the central limit theorem.

B. Neutral granular gases

For three-dimensional granular gases, we define the temperature

$$\frac{3}{2}T = \frac{1}{2}m\langle u^2\rangle \tag{5}$$

which is directly proportional to the second moment of the velocity distribution. The definition of the granular gas temperature effectively sets $k_B = 1$ as now temperature has units of energy. Due to the dissipative nature of the collisions it can be shown [6] that this quantity decreases in time according to Haff's law

$$T(t) = T_0(1 + t/\tau_0)^{-5/3} \tag{6}$$

for viscoelastic gases. One can therefore identify two timescales $\tau_v = \frac{m}{\gamma}$ and τ_0, which are the velocity relaxation and cooling time respectively. If $\tau_0 \gg \tau_v = \frac{m}{\gamma}$ so the timescales are well separated, the gas will evolve adiabatically. This means that at each point in time the granular gas is in local equilibrium at temperature $T(t)$, i.e. the change in $T(t)$ is slow enough for the gas to attain quasi-equilibrium.

Assuming $\gamma(u,t) = \gamma(t)$ and using the fluctuation-dissipation relation in 3D which holds for white noise and adiabatic evolution due to quasi-equilibrium

$$\Gamma = 6T\gamma \tag{7}$$

we obtain scaled Brownian motion using Haff's law for $T(t)$ and the self-diffusion relation $\gamma \propto \sqrt{T}$ [6, 17]. The resulting Langevin equation with time-dependent coefficients has been computed [7, 8] and shows very good agreement with event-driven neutral granular gas MD simulations.

C. Coulomb interactions

Charged granular gases involve long-ranged Coulomb interaction, which complicate matters as the particles no longer travel in ballistic trajectories between contact collisions. One therefore cannot use event-driven simulations, and it is a priori not clear whether a Langevin approach could work at all. The ranged correlations introduced by Coulomb interactions may require us to generalize the Langevin equation to coloured noises, work with a speed-dependent γ, or redefine the damping term with a memory kernel [18]. Figure 3 shows from MD force data that relation (4) holds well even in the charged case for our observation timescale, which rules out the need for a coloured noise term approach.

Our simulations use stochastic charge exchange as described in [19], where it is shown that the charge distribution of granules becomes stationary very early on during the evolution, albeit with fluctuations. Therefore, a reasonable place to start is Coulomb scattering. Let us consider two particles with initial velocities $\mathbf{v}_1$ and $\mathbf{v}_2$, and post-scattering velocities $\mathbf{v}_1'$ and $\mathbf{v}_2'$. The incoming velocities are assumed to be uncorrelated which is analogous to the molecular chaos hypothesis in the Boltzmann equation for dilute molecular gases [20]. From classical Coulomb scattering with scattering angle χ', impact parameter b and unperturbed incoming speed v_∞ of the first particle with charge q_1 as viewed in the frame of the second scatterer particle

$$\cot\left(\frac{\chi'}{2}\right) = \frac{\mu b v_\infty^2}{A} = a(b)v_\infty^2 \tag{8}$$

where $A = q_1q_2/(4\pi\epsilon_0)$ and $\mu = m/2$ is the reduced mass of the first particle. In this frame standard scattering coordinates (b,ϕ) describe the process [21].

Because v_∞ is the speed in the scatterer's frame, we can relate it to the lab frame where the scatterer velocity is $\mathbf{v}_2$ through a Galilean transformation $\mathbf{v}_1 = \mathbf{v}_\infty + \mathbf{v}_2$. By definition of the granular gas temperature (5) and the above assumption of uncorrelated velocities one obtains

$$\langle v_\infty^2\rangle_2 = v_1^2 + \frac{3T}{m} \tag{9}$$

where $\langle\rangle_2$ denotes the ensemble average over all the scatterer particles, for some given $\mathbf{v}_1$. What this equation tells us is

that the interaction with a generally moving background of scattering particles tends to increase v_∞ compared to v_1 due to the random thermal motion.

To proceed analytically, we could introduce an effective stationary background of fixed charges which captures the interaction with the true charged gas. By setting $v_2' = v_2 = 0$ one obtains the scattering angle in the lab frame $\chi = \chi'$. It can be immediately deduced that the change in velocity parallel to the incoming direction, denoting $\mathbf{u} = \mathbf{v}_1 = \mathbf{v}_\infty$, is

$$\Delta u_\parallel = u[\cos(\chi) - 1] = -2u[1 + a^2u^4]^{-1} \tag{10}$$

For this setup, the ensemble-average is now over the random scatterers like in (9) for a given incoming particle with velocity $\mathbf{u}$, since we want to determine the dynamical friction it experiences. $\langle \Delta u_\perp \rangle$ is zero due to the random angle ϕ, and this leads to a systematic drag force parallel to the initial velocity

$$m\left\langle \frac{\Delta u_\parallel}{\Delta t} \right\rangle = m\frac{\Delta x}{\Delta t} n \int_0^{2\pi} d\phi \int_{b_{min}}^{b_{max}} b\, db \frac{-2u}{1 + a^2u^4} \tag{11}$$

which we identify as $-|\gamma \mathbf{u}|$. The charge in general is distributed continuously and is problematic for obtaining an analytic expression in the ensemble average. Instead, we take a mean-field approach and treat each scattering process with the ensemble-averaged charge $q = \langle q_i^2 \rangle^{1/2}$, leading to $A = q^2/(4\pi\epsilon_0)$ in expressions (11) and similar. n is the local density and $n\Delta x/\Delta t = nu$ so that it represents the incoming flux of particles onto the scatterer. One can integrate the above expression to obtain

$$\gamma = \frac{4\pi A^2 n}{mu^3} \ln\left[\frac{1 + a_{max}^2 u^4}{1 + a_{min}^2 u^4}\right] \tag{12}$$

The integral over the impact parameter contains finite cutoffs in the integration limits, to prevent the integral from diverging. By modeling many-body Coulomb collisions as a succession of binary Coulomb collisions, one needs to introduce such cutoffs familiar to plasma physics [22]. Physically, the impact parameter cutoffs are related to the granule size and spacing.

Defining the Debye length and plasma frequency

$$\lambda_D = \sqrt{\frac{\epsilon_0 T}{nq^2}}, \quad \omega_p = \sqrt{\frac{nq^2}{\epsilon_0 m}} \tag{13}$$

respectively, we obtain

$$\gamma_C(u,t) = \frac{\omega_p m}{4\pi n \lambda_D^3} \ln[\Lambda(u)] \left(\frac{T}{mu^2}\right)^{3/2} \tag{14}$$

where we have defined the speed-dependent Coulomb integral

$$\Lambda(u) = \frac{1 + a_{max}^2 u^4}{1 + a_{min}^2 u^4} \tag{15}$$

Note that T is the temperature as defined in (5). In fact (15) is very similar to the dynamic friction coefficient in plasmas [23], but we have worked through the exact Coulomb scattering to obtain a well-defined expression for all u. In gravitational systems such as a dilute collection of stars, the $1/r$ potential leads to a similar expression for the dynamical friction experienced by a test mass [24]. The signed nature of Coulomb interactions does not qualitatively change the behaviour.

For speeds $u \gg (\frac{\langle q^2 \rangle}{4\pi\epsilon_0 dm})^{1/2}$ the deflections by Coulomb interactions will be negligible and the rate of contact collisions dominates, hence we expect a similar friction coefficient to the neutral gas, $\gamma_N(t) = \gamma_0(1 + t/\tau_0)^{-5/6}$ [8]. This observation suggests the following form

$$\gamma(u,t) = \gamma_C(u,t) + \gamma_N(t) \tag{16}$$

and represents our theoretical prediction for the speed-dependent friction coefficient. Note in the $u \to 0$ limit $\gamma_C \to 0$ and the neutral gas coefficient is recovered again. This intuitively makes sense as now deflection angles are large and repulsive interactions act effectively as contact collisions.

III. Methods

A. MD simulations

The granular gas MD simulation follows the model in [19] for viscoelastic collisions with ranged Coulomb interactions. Hertzian elastic contact forces as well non-linear dissipative contact forces are considered [25, 17]. The force of particle j on particle i has magnitude

$$\mathbf{F}_{ij}^N = \left(k_1 x_{ij}^{3/2} - k_2 x_{ij}^{1/2} \frac{dx_{ij}}{dt}\right) \mathbf{n}_{ij} \tag{17}$$

in the direction $\mathbf{n}_{ij} = (\mathbf{r}_i - \mathbf{r}_j)/|\mathbf{r}_i - \mathbf{r}_j|$. Here $x_{ij} = d - |\mathbf{r}_i - \mathbf{r}_j|$ denotes the compression between two colliding spheres, and the positive constants k depend on system parameters. Due to their contact nature, the forces only act when $x_{ij} > 0$. The exponents above can be corroborated with dimensional analysis [6]. To minimize finite-size effects, periodic boundary conditions are imposed meaning the system has infinite copies along each Cartesian axis. The Coulomb force

$$\mathbf{F}_{ij}^C = k_e \frac{q_i q_j}{(\mathbf{r}_i - \mathbf{r}_j)^2} \mathbf{n}_{ij} \tag{18}$$

is computed using the Ewald summation technique [26] which splits the sum into real and Fourier space parts to capture both short and long range effects accurately. Initially, particles start without any charge but the collisional charging mechanism based on empirical observations from [11] causes charge build-up, with the restriction of overall charge neutrality. Charge transfer is modelled to be proportional to some power of the relative kinetic energy

$$q_{i\to j} \propto \pm \left[\frac{m_{eff}}{2}\left(\frac{dx_{ij}}{dt}\right)^2\right]^\kappa \tag{19}$$

with stochasticity introduced in κ and the proportionality constant. Note $q_{j\to i} = -q_{i\to j}$. The overall code used for integration of the equation of motion is optimized to run on parallel graphics processing units (GPUs) and written in CUDA C. For a detailed description of the model employed, see section II in [19].

In MD simulations all numerical output data is in units of the reference quantities m, t_{ref}, d, $v_{ref} = d/t_{ref}$ and q_{ref} respectively. Note that the Coulomb coupling $k_e = 1/(4\pi\epsilon_0)$ is for the electric permittivity in free space.

Quantity	Value
mass m	$1.52 \cdot 10^{-4}$ kg
temperature T_0	$1.0 \cdot 10^{0}$ J
diameter d	$4.78 \cdot 10^{-3}$ m
Coulomb coupling k_e	$8.98 \cdot 10^{9}$ $\mathrm{F}^{-1}\,\mathrm{m}$
viscoelastic factor A	$1.86 \cdot 10^{-6}$ s
material/geometric constant ρ	$1.75 \cdot 10^{9}$ $\mathrm{Pa\,m}^{1/2}$
v_{ref}	$8.12 \cdot 10^{1}$ $\mathrm{m\,s}^{-1}$
t_{ref}	$5.88 \cdot 10^{-5}$ s
q_{ref}	$5.16 \cdot 10^{-6}$ C

TABLE I: Granular gas input parameters.

The (small) inelasticity is modeled here as

$$\epsilon = 1 - C_1 \kappa^{2/5} A g^{1/5} + \mathcal{O}(A^2 \kappa^{4/5} g^{2/5}) \tag{20}$$

which can be justified by dimensional analysis [6]. g is the normal component of the relative impact velocity at the time the particles start touching. Here all colliding particles have identical radii and masses. $\kappa = (3/2)^{5/2}(2\frac{\rho}{m})$ where ρ is

$$\rho = \frac{Y\sqrt{d}}{3(1-\nu^2)} \tag{21}$$

containing material parameters Young's modulus Y and Poisson's ratio ν.

From the kinetic theory of neutral viscoelastic gases [6] one can estimate for small inelasticities the cooling time

$$\tau_0^{-1} = \frac{64\pi^{\frac{1}{2}}}{5}\left(\frac{3}{2}\right)^{\frac{3}{5}} A q_0 d^2 n \left(\frac{T_0}{m}\right)^{\frac{11}{10}} \left(\frac{2\rho}{m}\right)^{\frac{2}{5}} g_2(d) \tag{22}$$

where $g_2(d) \approx 1$ is related to the two-particle correlation function and $q_0 \approx 0.173$ a value related to kinetic integrals. It is then calculated that $\tau_0^{-1} = 5.6 \cdot 10^3$ with parameters values from Table I. In terms of MD simulation time, $\tau_0^* = \tau_0 / t_{ref} = 3.0$ in this case.

B. Computation of the friction coefficient

Equation (3) provides us with a method to estimate the numerical value of $\gamma(u,t)$ from our MD simulation data. By computing the speeds of all particles and ordering them into bins corresponding to sufficiently small speed intervals, the speed-restricted ensemble average can be performed over the bin size. To study potential power law relations between γ and u a log-log plot is used. The corresponding intervals of speed were thus taken to scale exponentially. Based on the theoretical prediction (14) a plot against u/σ_u could be fruitful, so we bin the speed according to boundaries $u_i = k^i \sigma_u$ for integer i and some constant k which results in a sufficiently fine partition of the $\log(u/\sigma_u)$ axis. Due to finite ensemble size in our simulation, k should not be too small as fluctuations will become more dominant in each bin. To retain statistically reasonable results, only bins with more than $\frac{1}{10}$ of the highest bin frequency were plotted. We have now discretized (3) into

$$\gamma(u_i,t) \approx -\frac{\langle \boldsymbol{u}(t)\cdot\boldsymbol{F}(t)\rangle_{u_i<u<u_{i+1}}}{\langle \boldsymbol{u}(t)\cdot\boldsymbol{u}(t)\rangle_{u_i<u<u_{i+1}}} \tag{23}$$

and this can be computed at various times to study its time evolution.

To model the theoretical expression (16) we need to compute it. Analytically, γ_C will tend to zero at zero speed but numerical computations may have issues with this limit at very small speeds. We thus Taylor expand in the very low speed limit in our numerical evaluation of $\gamma(u,t)$. The computational form used for $\gamma_C(u,t)$ is

$$\begin{aligned} \gamma_C &= H\left(\frac{3T}{m}\right)^{\frac{3}{2}}(C_{max}-C_{min})\cdot u, \quad C_{max}u^4 \le C_c \\ \gamma_C &= H\left(\frac{3T}{mu^2}\right)^{\frac{3}{2}} \ln\left[\frac{1+C_{max}u^4}{1+C_{min}u^4}\right], \quad C_{max}u^4 > C_c \end{aligned} \tag{24}$$

where we introduced new constants to characterize the function. C_c was chosen to be 10^{-10}. In principle the parameters H, C_{max} and C_{min} can be deduced by fitting to computation of (23) as shown in Figure 2.

From these results, we see our MD gas should be evolving adiabatically, since $\tau_0 \gg \tau_v = \frac{m}{\gamma}$ holds for computed values of γ. τ_0 is taken to be the value deduced by fitting in Figure 2.

C. Finite difference equation

To numerically solve the stochastic Langevin equation a finite difference approach is used similar to [27]. We discretize equation (1) using the following definitions with $\Delta x_n = x_{n+1} - x_n$ and a fixed time interval $\Delta t = t_i - t_{i-1}$

$$\begin{aligned} \frac{dx(t)}{dt} &\to \frac{\Delta x_{i-1}}{\Delta t} = \frac{x_i - x_{i-1}}{\Delta t} \\ \frac{d^2x(t)}{dt^2} &\to \frac{\Delta x_{i-1} - \Delta x_{i-2}}{(\Delta t)^2} = \frac{x_i + x_{i-2} - 2x_{i-1}}{(\Delta t)^2} \end{aligned} \tag{25}$$

which is consistent with the non-anticipatory nature of the stochastic process. Note it is an implicit algorithm in Δx_i making it numerically stable for large γ values.

To discretize the white Gaussian noise we employ the approximation $\int_{t_i}^{t_i+\Delta t} dt' \xi_x(t') \approx \xi_{x,i}\Delta t$ and apply it to (4) to see that $\langle \xi_{x,i}\xi_{x,j}\rangle (\Delta t)^2 = \Gamma(t_i)\delta_{ij}\Delta t$ which allows us to identify $\xi_{x,i}$ with a normally distributed random variable

$$\xi_x(t) \to \xi_{x,i} = \mathcal{N}\left(0, \frac{\Gamma(t_i)}{\Delta t}\right) = \sqrt{\frac{\Gamma(t_i)}{\Delta t}}\mathcal{N}(0,1) \tag{26}$$

In order to make the discrete equation tractable we use a slightly different definitions for the speed in $\gamma(u,t)$

$$u(t) \to \frac{[(\Delta x_{i-2})^2 + (\Delta y_{i-2})^2 + (\Delta z_{i-2})^2]^{1/2}}{\Delta t} \tag{27}$$

which allows us to solve components at i in terms of $i-1$ and $i-2$ components leading to the recursion relation

$$\begin{aligned} x_i &= \frac{(\alpha+2)x_{i-1} - x_{i-2} + \beta * \mathcal{N}(0,1)}{\alpha+1} \\ \alpha &= \frac{\gamma(u_i,t_i)\Delta t}{m}, \quad \beta = (\Delta t)^{\frac{3}{2}}\sqrt{\Gamma(t_i)}/m \end{aligned} \tag{28}$$

which is our final finite difference equation. The same results hold for y and z components. It is essentially the Euler-Maruyama integration algorithm [28], which allows a consistent treatment of the noise term $\boldsymbol{\xi}(t)$.

To obtain reasonably accurate numerical solutions, the time step Δt should be smaller than $\tau_v = \frac{m}{\gamma}$ which represents the timescale over which initial conditions in velocity decay away.

Lastly, the initial conditions used for the particles is starting at the origin with zero velocity. To contrast with the MD simulation model, the gas is initialized by computing a neutral elastic evolution to attain an equilibrium Maxwell distribution in velocity space and a homogeneous space distribution before the start of data extraction.

IV. Results

In this study, our results are grouped into two classes: MD simulation results and computation of the finite difference equation. To compare the two results we iterate here that the MD output data is dimensionless as explained in section III with reference quantities given in Table I. For example the dimensionless time quantities $t^* = t/t_{ref}$, using the $*$ to denote these quantities. Correspondingly, we can derive from dimensional analysis the following relations for the friction coefficient and the granular temperature

$$\begin{aligned} \gamma^* &= \gamma \frac{t_{ref}}{m} \\ T^* &= T \frac{t_{ref}^2}{md^2} \end{aligned} \tag{29}$$

In the following figures of this section for notational convenience, all quantities have numerical values in these dimensionless system of units to allow direct comparison of the MD and finite difference computation results. All quantities should be interpreted as the starred quantities.

One key quantity computed was the ensemble-averaged mean squared displacement (MSD)

$$\langle R^2 \rangle = \langle (\mathbf{x}(t) - \mathbf{x}_0)^2 \rangle = \frac{1}{N} \sum_{i=1}^{N} [\mathbf{x}^{(i)}(t) - \mathbf{x}^{(i)}(0)]^2 \tag{30}$$

with $\mathbf{x}^{(i)}$ the single-particle trajectory for particle i. Increasing the ensemble size will reduce fluctuations and lead to smoother MSD functions.

A. MD simulations

Four independently initialized MD simulations in three dimensions for the charged gas and six for the neutral gas were run, each with $N = 50016$ particles. The box length is $L_{cell} = 70$. This allows us to compute properties of the gas from a large particle ensemble, reducing fluctuations in the results. In a similar fashion, we can calculate other ensemble-averaged quantities as the granular gas temperature using the single-particle trajectories.

1) Generalized friction coefficient: Computation of (23) shows that

$$\gamma^*(u,t) \approx \left(C \left(\frac{u}{\sigma_u(t)} \right)^{-3} + \gamma^*_\infty(t) \right) \tag{31}$$

for some time-independent constant C and some time-dependent asymptotic high speed value $\gamma_\infty(t)$. Figure 2 shows the computed values as scatter points. The bin size is such that the speed axis was divided into 10 equal segments on the log plot. Indeed, the u^{-3} dependence predicted by Coulomb scattering and known for plasmas [23] supports our approach in section II. For neutral gases, speed independence of γ seems to agree with most computed bins as expected, although the low velocity tail does show a similar relation to the charged gas. However, we need to be careful as the number of particles in the speed regimes at the tail of the distribution are lower and the results are much more prone to fluctuations.

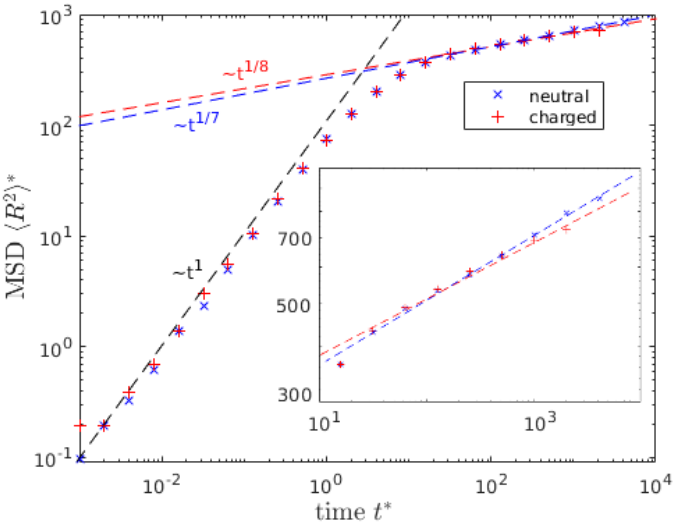

Fig. 1: Ensemble-averaged MSD against time from the MD data for the granular gas, with power laws fitted to indicate time scalings. The long time power laws were fitted to the last 6 data points, and the more precise expression for the neutral power is $\frac{139}{1000}$.

The constant $C = \frac{t_{ref} H}{m} \ln[\frac{C_{max}}{C_{min}}]$ when compared to (24), since we are in the high u limit where $C_{max} u^4 \gg 1$. Comparison with MD data in Figure 2 suggests $C \approx 10^{-5}$. Also, the form $\gamma^*_\infty(t) \approx 10^{-1}(1 + t/\tau_o)^{-5/6}$ holds as time evolves, although with relatively large fluctuations originating from the reduced particle numbers at the high-speed tail. This result supports the previous intuitive deduction for the high speed limit of γ. Additionally, the lack of very low-speed particles means the region around the presumed peak of γ has not been accessed. $C_{max/min}$, which shift the peak, are therefore not determined by these results. Compared with the theoretical form (16), (31) is compatible and implies $\frac{\omega_p m}{n \lambda_D^3}$ is a constant in time, at least for the observed time frame. Additionally in this high u limit $\ln[\Lambda(u)] \approx 2 \ln[a_{max}/a_{min}]$, which is a constant independent of u/σ_u, seems to hold for the range of computed scatter points.

2) MSD: From the observed long-time MSD from MD simulations, charged granular gases seem to have a slightly more subdiffusive character than neutral gases ($\propto t^{1/8}$ rather than $\propto t^{1/6}$, although in Figure 1 the neutral long time exponent seemed to be around $\frac{1}{7}$). Note the ballistic regime was not observed in our time frame.

3) Noise properties: Computing (4) for our MD data shows that the noise term is indeed well-approximated by white noise in charged gases, at least for our observation timescale. The delta correlation in (4) is idealized and was observed in Figure 3 as a sharp peak in simulation where we have discretized time. The same was observed for neutral gases and that justifies computationally the use of white noise in the Langevin approach as done in [8]. Note that to compute ξ

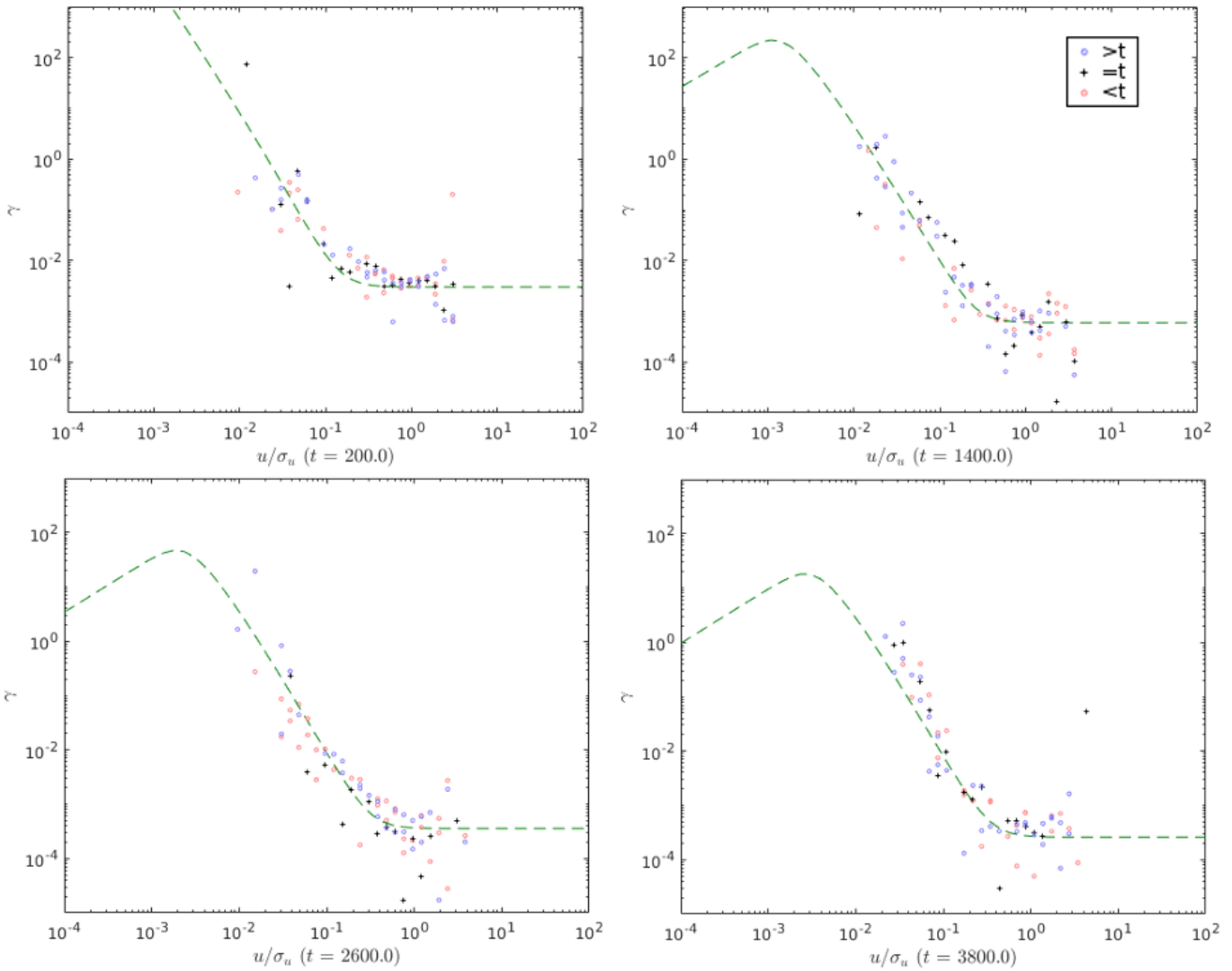

Fig. 2: Computation of (23) from the charged gas MD data at various times t shown as scatter points. The theoretical fit (24) is depicted by the green dashed line. Scatter points fluctuate in time about the fitted curve, but overall there seems to be a consistent agreement for the available speed range. Fluctuations in time are conveyed through plotting scatter points taken from data at $t \pm 1$ and $t \pm 2$. Crosses represent data at the given time t. Note that t and $gamma$ in the plot are in dimensionless simulations (starred) units. The parameters used for the fit are $\tau_0 = 3.0$, $\gamma_0 = 10^{-1}$, $C_{max} = 10^{12}$, $C_{min} = 10^4$ and $H = 10^{-5} \ln(C_{max}/C_{min})$.

from (2) we use the speed-dependent γ from (24) with fitted parameters as shown in Figure 2 for the charged case. Force data were extracted every 1000 computation steps, which corresponds to output every integer time t^* which coarse-grained our results.

When looking at the total force split into Hertian elastic, dissipative, and Coulomb as defined in (17) and (18), the correlations between the components as well as self-correlations show coloured behaviour. In particular, the Coulomb and Hertzian elastic force become more negatively correlated as the gas evolves. Remarkably, the stochastic noise term related to the total force shows white noise characteristics discussed previously as these correlations cancel each other out. The cancellation is not perfect though and leads to small correlations around the peak in Figure 3.

From (4) it is expected that $\Gamma(t)$ is proportional to the variance of the noise computed for the discretized MD simulation data. Figure 4 shows the noise variance $\sigma_\xi^2 \propto (1 + t/\tau_0)^{-5/2}$ and again the same was observed for the neutral counterpart. In the latter case, this result is consistent with the fluctuation-dissipation relation (7) showing that indeed $\Gamma(t) \propto \sigma_\xi^2(t)$.

The probability distribution characterizing the noise was also estimated from the available MD force data at a given time t, and it is not Gaussian. Instead, the form seems to be

$$P_\xi \propto \exp\left(-\frac{|\xi|}{a\sigma_\xi(t)}\right) \tag{32}$$

where a is some constant which varies slowly with time.

4) Haff's law: It is observed that Haff's law $\frac{3}{2}T = \frac{1}{2}m\sigma_u^2 \propto (1 + t/\tau_0)^{-5/3}$ holds well in both cases in our MD simulations. This is intuitively expected as the charged gas has zero net charge [19]. Figure 5 shows the data for the charged case, where $t^* \approx 1000$ seems to deviate from the prediction. This is due to the presence of macroscopic fluxes [6] as clustering takes place.

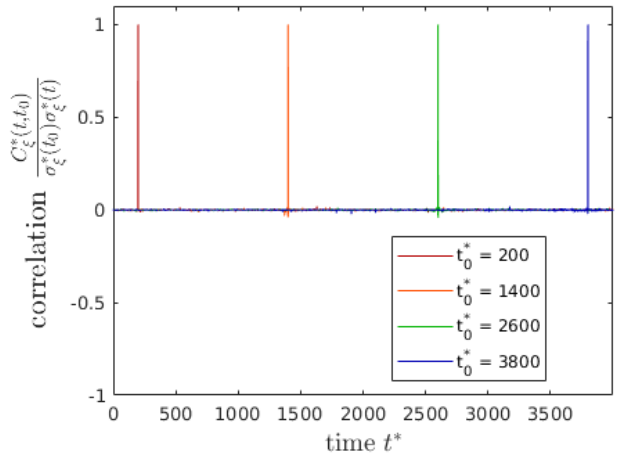

Fig. 3: Self-correlation of $\xi_x(t)$ computed from MD data for the charged gas. Note the very small correlations that develop around the peak at later times.

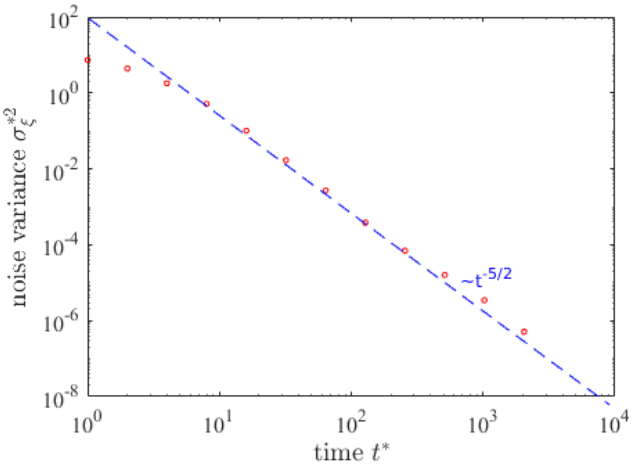

Fig. 4: The variance of the noise term $\xi_x(t)$ in the charged gas plotted against time, defined as $\sigma_\xi(t) = \langle \xi_x(t)\xi_x(t)\rangle$.

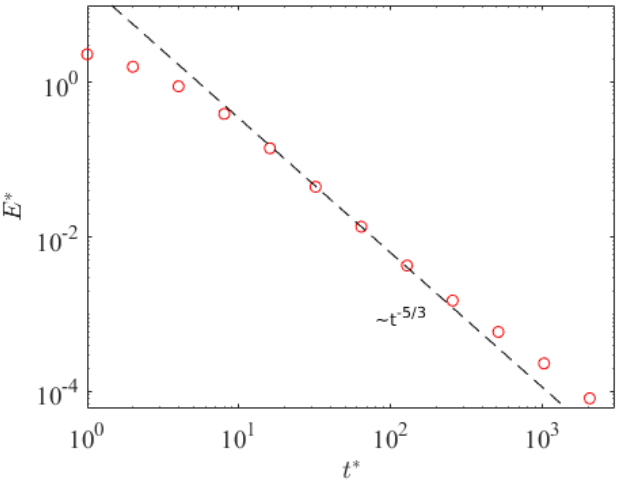

Fig. 5: The kinetic energy of the charged gas $E = \frac{3}{2}T = \frac{1}{2}m\langle u^2\rangle$ plotted against time, showing agreement with Haff's law.

B. *Finite difference equation*

The ensemble size used in the finite difference equation is $N = 100$ particles.

1) MSD time scaling: Our finite difference equation reduces to the neutral gas case when $\gamma_C = 0$ and computation of the ensemble-averaged MSD shows results which agree with established observations in literature [8]. In Figure 6 we indeed observe this is the case for our integration scheme, validating its accuracy for these set of parameters.

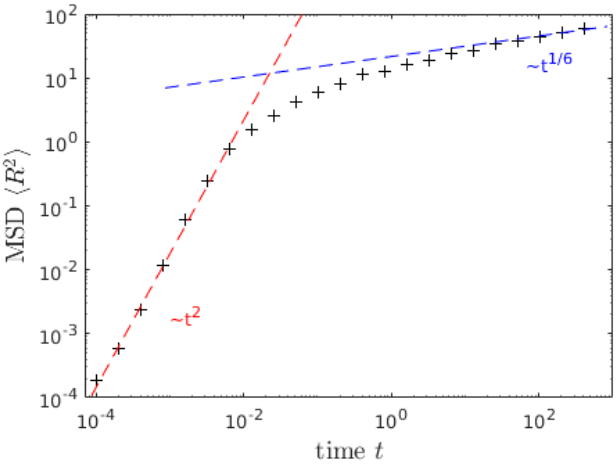

Fig. 6: Ensemble-averaged MSD against time, the coloured lines represent power law scalings with time computed for the neutral gas. Light blue is t^2, red is t^1, blue is $t^{1/6}$, green is $t^{1/8}$. The MSD seems to tend to the $t^{1/6}$ scaling. Parameters used have numerical values of $\Delta t = 10^{-5}$, $T_0 = 1.0$, $m = 1.52 \cdot 10^{-4}$, $\gamma_0 = 10^{-1}$, $\tau_0 = 10^{-2}$.

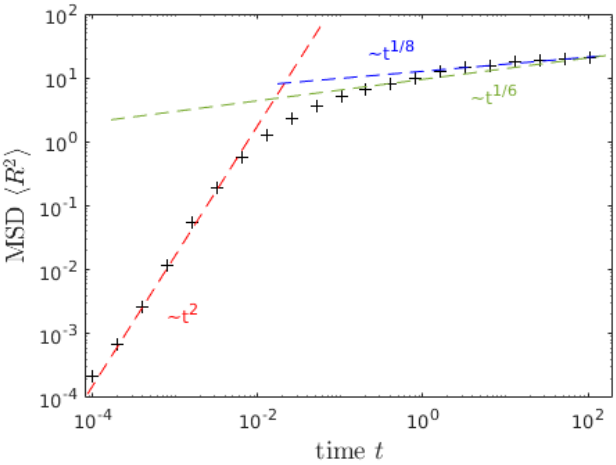

Fig. 7: Ensemble-averaged MSD against time, the coloured lines represent power law scalings with time. Light blue is t^2, red is t^1, blue is $t^{1/6}$, green is $t^{1/8}$. The MSD seems to tend to the $t^{1/8}$ scaling. Parameters used had numerical values of $\Delta t = 10^{-3}$, $T_0 = 1.0$, $m = 1.52 \cdot 10^{-4}$, $\gamma_0 = 10^{-1}$ and $\tau_0 = 10^{-2}$, $C_{max} = 10^{12}$, $C_{min} = 10^3$, $H = 10^{-5}\ln(C_{max}/C_{min})$.

Turning on the charge interaction, the same was done with results Figure 7, showing a more subdiffusive trend at long times. To compare with MD simulations, we have rescaled the input parameters and variables of the finite difference equation

following the process in (29) to match MD input parameters. The plot computed is shown in Figure 8. It does not agree quantitatively with the MD plot Figure 1, but again it does show the charged case is more subdiffusive.

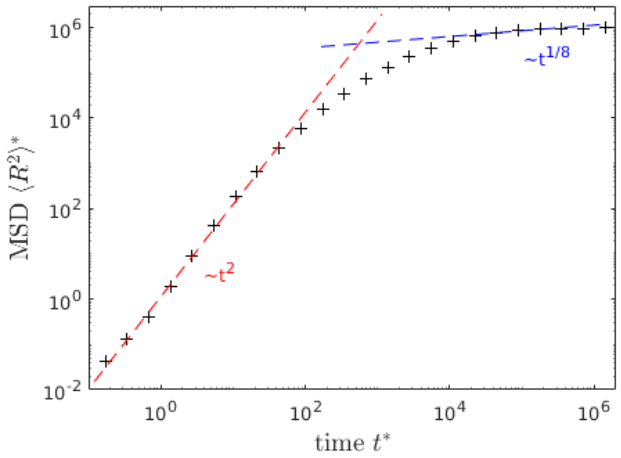

Fig. 8: Ensemble-averaged MSD against time, the coloured lines represent power law scalings with time. Light blue is t^2, red is t^1, blue is $t^{1/6}$, green is $t^{1/8}$. The MSD seems to tend to the $t^{1/8}$ scaling, with a zoom in provided in the right bottom corner. Parameters used had numerical values of $\Delta t = 10^{-5}$, $T_0^* = 1.0$, $m^* = 1.0$, $\gamma_0^* = 10^{-1}$ and $\tau_0^* = 3.0$, $C_{max} = 10^{12}$, $C_{min} = 10^4$, $H = \frac{m}{t_{ref}} 10^{-5} \ln(C_{max}/C_{min})$. The scaled parameters are defined with respect to gas input parameters Table I.

2) Granular gas temperature: Another aspect of the Langevin equation to check is the time dependence of the temperature as defined in (5) which is shown in Figure 9 and Figure 10, which correspond to the same data shown in the MSD plots before. Indeed, it seems to agree with Haff's law meaning the second moment of the velocity distribution in the Langevin model is reasonably comparable with the kinetic theory.

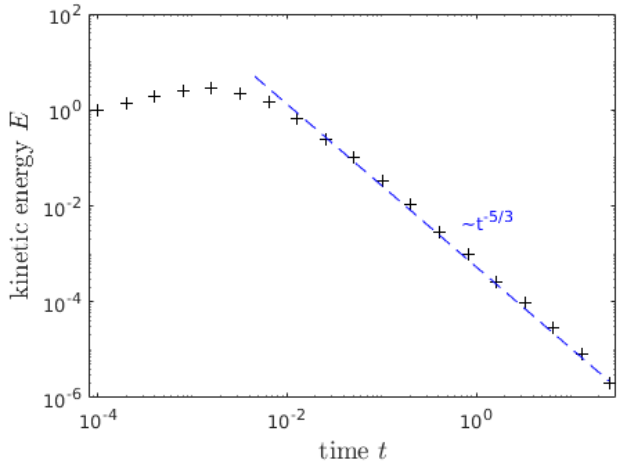

Fig. 9: Ensemble-averaged granular gas kinetic energy E against time t for the data presented in Figure 7. The blue fit is $\propto t^{-5/3}$ which is the asymptotic limit of Haff's law for neutral viscoelastic gases.

V. Discussion

A. Adiabaticity

The adiabatic condition $\tau_0 \gg m/\gamma$ in our MD simulations is not necessarily satisfied for early times as one can check with the gas parameters in Table I. It turns out that $\tau_0^* \approx 3$ whereas $\tau_v^* \approx 10^1$ for $\gamma = \gamma_N$ at $t = 0$ and this velocity relaxation time will only get bigger at later times. However lower speed particles have significant contribution from γ_C and these will lower τ_v. For the corresponding neutral MD gas, this observation of non-adiabatic evolution could explain why we observed a slightly different long-time exponent in Figure 1 compared to theory.

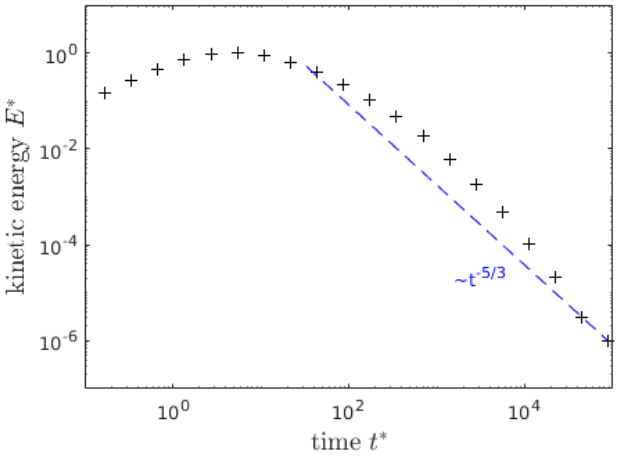

Fig. 10: Ensemble-averaged granular gas kinetic energy E against time t for the data presented in Figure 8. The blue fit is $\propto t^{-5/3}$ which is the asymptotic limit of Haff's law for neutral viscoelastic gases.

B. Initial conditions

Our Langevin approach has different initial conditions from the MD simulations. MD simulations start out with a Maxwellian velocity distribution, whereas the Langevin equation was solved with zero initial velocity. An initial Maxwellian distribution of temperature T_0 can be easily incorporated into the finite difference equation, and the results had no effect on the long-term behaviour which is expected as initial conditions are washed out over the timescale τ_v.

C. Relation with plasma physics

Usage of Coulomb scattering in deriving γ connects to plasma physics, but this analogy has its limitations. Collide-and-capture events observed in simulations as well as in real granular systems [19, 15] suggest that the actual scattering process involves compound particles rather than separate particles. The charges and masses can therefore be different from the single particle properties, and the constants in (14) and elsewhere should be treated as effective constants. Highly charged particles will tend to be surrounded by opposite charges and thus these compound particles will have a suppressed overall charge.

As mentioned in section IV, $\frac{\omega_p m}{n\lambda_D^3}$ seems to be time-independent. These quantities do not necessarily refer to the single particle properties as discussed in the above paragraph. Physically, λ_D is the length scale over which Coulomb interactions are shielded away significantly. This is derived under the assumptions of thermal equilibrium so a Boltzmann distribution holds, and small electrostatic energies compared to thermal energy T [29]. From our simulation, the average absolute charge and the Coulomb force magnitude seem to remain reasonably constant (simulation time $t_{end} = 3000$) while the thermal energy decays. This expression therefore ought to be interpreted with care.

Lastly, the approximation of a stationary scattering background needs to be taken with a grain of salt. Equation (10) clearly shows that especially near thermal velocities, one expects a significant influence from the thermal background motion. In Figure 2 we have noticed the absence of particles in the very low speed regime (below $u/\sigma_u \approx 10^{-2}$, and is likely to be directly related. Our approach leading to the generalized Langevin equation does not reduce the accessibility of low speed regimes in itself.

D. Coulomb interaction strength

Future studies could investigate the dependence of γ_C on the Coulomb interaction strength in our granular gas system. Rescaling k_e effectively modifies the charge exchange strengths and correspondingly the ratio of the typical Coulomb to the kinetic energy. A previous study [19] has noted that the onset of clustering takes places earlier as Coulomb strength is increased, but surprisingly it does not affect the average cluster size growth exponent. Varying the Coulomb interaction strengths could show interesting scaling behaviour of parameters, which in turn may elucidate more of the underlying kinetic and collective processes.

VI. Conclusion

We generalized the Langevin approach for self-diffusion in viscoelastic granular gases to describe single-particle trajectories for charged granular gases. Our approach is based on introducing a speed-dependent dynamical friction coefficient, which also emerges in other systems with $1/r$ potential interactions such as plasmas. MD simulations support the functional form of the friction coefficient derived from Coulomb scattering and the self-diffusion relation in viscoelastic gases.

Using the MD simulation data, we have also shown agreements with the white noise assumption (4) and the fluctuation-dissipation relation (7) used in the Langevin approach for neutral gases.

The finite difference equation provided a discretization of the resulting Langevin equation, which was numerically solved for single-particle trajectories. From there, the ensemble-averaged mean square displacement was computed and indicated slightly more subdiffusive behaviour in the long time limit for the charged case compared to the neutral gas.

References

[1] Kevin Lu, E. E. Brodsky, and H. P. Kavehpour. A thermodynamic unification of jamming. *Nature Physics*, 4:404 EP –, Apr 2008.

[2] R. Greenberg, R.J. Greenberg, A. Brahic, and M.S. Matthews. *Planetary Rings*. Space science series. University of Arizona Press, 1984.

[3] J. Duran. *Sands, Powders and Grains*, volume 1. Springer, 2000.

[4] Mathias Hummel and Marco G Mazza. Declustering in a granular gas as a finite-size effect. *Phys. Rev. E*, 93(2):022905, 2016.

[5] S Miller and S Luding. Cluster growth in two-and three-dimensional granular gases. *Phys. Rev. E*, 69(3):031305, 2004.

[6] Nikolai V. Brilliantov and Thorsten Pöschel. *Kinetic theory of granular gases*. Oxford University Press, 2010.

[7] Anna Bodrova, Aleksei V Chechkin, Andrey G Cherstvy, and Ralf Metzler. Quantifying non-ergodic dynamics of force-free granular gases. *Phys. Chem. Chem. Phys.*, 17(34):21791–21798, 2015.

[8] Anna S Bodrova, Aleksei V Chechkin, Andrey G Cherstvy, Hadiseh Safdari, Igor M Sokolov, and Ralf Metzler. Underdamped scaled brownian motion:(non-) existence of the overdamped limit in anomalous diffusion. *Sci. Rep.*, 6:30520, 2016.

[9] Ralf Metzler, Jae-Hyung Jeon, Andrey G. Cherstvy, and Eli Barkai. Anomalous diffusion models and their properties: non-stationarity, non-ergodicity, and ageing at the centenary of single particle tracking. *Phys. Chem. Chem. Phys.*, 16:24128–24164, 2014.

[10] Thomas Pähtz, Hans J Herrmann, and Troy Shinbrot. Why do particle clouds generate electric charges? *Nature Physics*, 6(5):364–368, 2010.

[11] Torsten Poppe, Jürgen Blum, and Thomas Henning. Experiments on collisional grain charging of micron-sized preplanetary dust. *Astrophys. J.*, 533(1):472, 2000.

[12] Frank Spahn and Martin Seib. Charges dropped. *Nature Physics*, 11:709 EP –, Jul 2015.

[13] C D Stow. Dust and sand storm electrification. *Weather*, 24(4):134–144, 1969.

[14] V.A. Rakov and M.A. Uman. *Lightning: Physics and Effects*. Cambridge University Press, 2007.

[15] Victor Lee, Scott R Waitukaitis, Marc Z Miskin, and Heinrich M Jaeger. Direct observation of particle interactions and clustering in charged granular streams. *Nature Physics*, 11(9):733–737, 2015.

[16] René Weidling and Jürgen Blum. Free collisions in a microgravity many-particle experiment. iv.–three-dimensional analysis of collision properties. *Icarus*, 253:31–39, 2015.

[17] Nikolai V Brilliantov, Frank Spahn, Jan-Martin Hertzsch, and Thorsten Pöschel. Model for collisions in granular gases. *Phys. Rev. E*, 53(5):5382, 1996.

[18] Denis S. Grebenkov and Mahsa Vahabi. Analytical solution of the generalized langevin equation with hydrodynamic interactions: Subdiffusion of heavy tracers. *Phys. Rev. E*, 89:012130, Jan 2014.

[19] Chamkor Singh and Marco G. Mazza. Early-stage aggregation in three-dimensional charged granular gas. *Phys. Rev. E*, 97:022904, Feb 2018.

[20] Byung Chan Eu. *Boltzmann Kinetic Equation*, pages 61–136. Springer International Publishing, Cham, 2016.

[21] Harald Friedrich. *Classical Scattering Theory*, pages 1–21. Springer Berlin Heidelberg, Berlin, Heidelberg, 2013.

[22] Robson R. E. *Introductory transport theory for charged particles in gases*. World Scientific, 2006.

[23] James D. Callen. *Fundamentals of Plasma Physics*. University of Wisconsin, 2006.

[24] Subrahmanyan Chandrasekhar. Dynamical friction. i. general considerations: the coefficient of dynamical friction. *The Astrophysical Journal*, 97:255, 1943.

[25] Thorsten Pöschel and Thomas Schwager. *Computational granular dynamics: models and algorithms*. Springer Science & Business Media, 2005.

[26] Daan Frenkel and Berend Smit. *Understanding molecular simulation: from algorithms to applications*, volume 1. Academic press, 2001.

[27] Giorgio Volpe and Giovanni Volpe. Simulation of a brownian particle in an optical trap. *American Journal of Physics*, 81(3):224–230, 2013.

[28] Peter E. Kloeden and Eckhard Platen. *Numerical Solution of Stochastic Differential Equations*. Springer Berlin Heidelberg, 1992.

[29] Pallab Ghosh. Electrostatic double layer force: Part ii.